

Electro-magneto-thermo-mechanical Behaviors of a Radially Polarized FGPM Thick Hollow Sphere

A. Ghorbanpour Arani^{*}, J. Jafari Fesharaki, M. Mohammadimehr, S. Golabi

Department of Mechanical Engineering, Faculty of Engineering, University of Kashan, Kashan, Islamic Republic of Iran

Received 25 September 2010; accepted 8 November 2010

ABSTRACT

In this study an analytical method is developed to obtain the response of electro-magneto-thermo-elastic stress and perturbation of a magnetic field vector for a thick-walled spherical functionally graded piezoelectric material (FGPM). The hollow sphere, which is placed in a uniform magnetic field, is subjected to a temperature gradient, inner and outer pressures and a constant electric potential difference between its inner and outer surfaces. The thermal, piezoelectric and mechanical properties except the Poisson's ratio are assumed to vary with the power law functions through the thickness of the hollow sphere. By solving the heat transfer equation, in the first step, a symmetric distribution of temperature is obtained. Using the infinitesimal electro-magneto-thermo-elasticity theory, then, the Navier's equation is solved and exact solutions for stresses, electric displacement, electric potential and perturbation of magnetic field vector in the FGPM hollow sphere are obtained. Moreover, the effects of magnetic field vector, electric potential and material in-homogeneity on the stresses and displacements distributions are investigated. The presented results indicate that the material in-homogeneity has a significant influence on the electro-magneto-thermo-mechanical behaviors of the FGPM hollow sphere and should therefore be considered in its optimum design.

© 2010 IAU, Arak Branch. All rights reserved.

Keywords: FGPM; Thick hollow sphere; Electro-magneto-thermo-mechanic; Perturbation of the magnetic field vector.

1 INTRODUCTION

FGPMs have attracted widespread attention in recent years. FGPM is a kind of piezoelectric material with material composition and properties that varies continuously and gradually along certain directions. This makes FGPM to be suitable for many specific applications such as sensors or actuators. Chen et al. [1] investigated a piezoceramic hollow sphere analytically, based on the 3D equations of mechanical and piezoelectricity. Their numerical results are performed for different boundary conditions imposed on the spherical surfaces. Lim and He [2] obtained an exact solution of a compositionally graded piezoelectric layer under uniform stretch, bending and twisting. Shi and Chen [3] presented the analytical solution for a piezoelectric cantilever beam with continuously graded properties subjected to different loadings. They proposed and determined a pair of stress and induction functions in the form of polynomials. Moreover, based on these functions, they obtained a set of analytical solutions for the beam under different loadings. WU and Syu [4] considered an exact solution of a cylindrical shell made of functionally graded piezoelectric materials under cylindrical bending using the method of perturbation. They are taken into account the transverse normal load and normal electric displacement (or electric potential), respectively, applied on the lateral surfaces of the shells. Moreover, they assumed that the cylindrical shells are considered to be

^{*} Corresponding author. Tel.: +98 9131626594 ; Fax: +98 361 5513011
E-mail address: aghorban@kashanu.ac.ir; a_ghorbanpour@yahoo.com (A. Ghorbanpour Arani).

fully simple supports at the edges in the circumferential direction and with a large value of length in the axial direction. Also, they investigated the coupled electro-elastic effect on the structural behavior of FG piezoelectric shells and the influence of the material property gradient index on the variables of electric and mechanical fields.

For an electro-magneto-elastic case, Dai et al. [5] studied the electro-magneto-elastic behaviors of functionally graded piezoelectric in geometry, i.e. solid cylinders and spheres. They showed that mechanical and electric loads on the FGPM cylinders and spheres can control the distributions of stresses, perturbation of magnetic field vector and electric potential in the FGPM solid structures. For an electro-thermo-elastic case, Ootao and Tanigawa [6] carried out the transient piezothermoelastic analysis for a hollow sphere made of functionally graded piezoelectric material. They considered the thermal, thermo-elastic and piezoelectric constants of the hollow sphere as power functions of the radial coordinate and showed some numerical results for the temperature change, displacement, stress and electric potential distributions. Khoshgoftar et al. [7] presented the thermo-elastic analysis of a thick walled cylinder made of functionally graded piezoelectric material. They loaded the cylinder subjected to the temperature gradient and inner and outer pressures and also defined all the mechanical, thermal and piezoelectric properties except the Poisson ratio as a power function in the radial direction. Ghorbanpour Arani et al. [8] considered a hollow circular cylinder made of exponentially graded piezoelectric material (EGPM), e.g. PZT₄. Their loadings were composed of internal and external pressures, a distributed temperature field due to steady state heat conduction with convective boundary condition, an inertia body force due to rotation with constant angular velocity and a constant electric potential difference between its inner and outer surfaces. Also, they assumed that the material properties except Poisson's ratio and thermal conduction coefficient are exponentially distributed along radius.

For a magneto-thermo-elastic case, by means of an analytical method, Ghorbanpour Arani et al. [9] investigated the magneto-thermo-elastic stress and perturbation of the magnetic field vector in functionally graded hollow sphere placed in uniform magnetic and temperature fields subjected to an internal pressure. They employed hypergeometric functions to solve the governing equation and also assumed that the material properties through the graded direction are nonlinear with an exponential distribution. Moreover, they obtained the temperature, displacement and stress fields and the perturbation of magnetic field vector and compared with those of the homogeneous case. Ghorbanpour Arani et al. [10] presented an exact solution for magneto-thermo-elastic transient response and perturbation of the magnetic field vector for a functionally graded thick hollow sphere subjected to magnetic and thermo-elastic fields. Using the Hankel and Laplace transform techniques, they solved the dynamic equation of magneto-thermo-elastic and the radial and circumferential stresses as well as the perturbation of the magnetic field vector for a typical material are obtained. For an electro-magneto-thermo-elastic case, Dai et al. [11] studied the electro-magneto-thermo-elastic behaviors of a functionally graded piezoelectric hollow cylinder, placed in a uniform magnetic field, subjected to electric, thermal and mechanical loads. Using the infinitesimal theory of electro-magneto-thermo-elasticity, they obtained the electric, magnetic, thermal and mechanical properties of the material that obey an identical power law in the radial direction and also determined exact solutions for electric displacement, stresses, electric potential and perturbation of magnetic field vector in the FGPM hollow cylinder.

In this study, an exact solution for a radially polarized FGPM hollow sphere with electro-magneto-thermo-elastic behaviors subjected to magnetic and thermo-elastic field is presented. The material properties through the graded direction are assumed to be nonlinear with a power law function. The temperature, displacement and stress fields, electric potential and the perturbation of magnetic field vector are determined and compared with those of the homogeneous case.

2 BASIC FORMULATIONS

2.1 Heat conduction equation

The axisymmetric, steady state, and heat conduction equation in the spherical coordinate system with the thermal boundary condition is given in this section as [8]

$$\frac{1}{r^2} \frac{\partial}{\partial r} \left[r^2 k(r) \frac{\partial T(r)}{\partial r} \right] = 0, \quad a \leq r \leq b \quad (1a)$$

$$T(r)|_{r=a} = T_o \quad (1b)$$

$$\left[\frac{\partial T(r)}{\partial r} + hT(r) \right] \Big|_{r=b} = 0 \quad (1c)$$

where a and b are the inner and outer radii, respectively, $k=k(r)$ is the thermal conductivity which is assumed to be a function of radius, h is the convective heat transfer coefficient ratio and T is the temperature. Assuming $k(r)$ as a function of radius:

$$k(r) = k_0 r^m \quad (2)$$

where k_0 is the nominal thermal conductivity, and m is the material in-homogeneity. Substituting Eq. (2) into Eq. (1a) yields the FGPM heat conduction equation as

$$\frac{1}{r^2} \frac{\partial}{\partial r} \left[r^{m+2} \frac{\partial T(r)}{\partial r} \right] = 0 \quad (3)$$

Integrating twice Eq. (3) yields

$$T(r) = C_1 r^{-m-1} + C_2 \quad (4)$$

Using the boundary conditions (1b) and (1c), the constants C_1 and C_2 are determined as follows

$$C_1 = \frac{-T_0 h}{hb^{-(m+1)} - (m+1)b^{-(m+2)} - ha^{-(m+1)}}, \quad (5)$$

$$C_2 = \frac{T_0 hb^{-(m+1)} - (m+1)T_0 b^{-(m+2)}}{hb^{-(m+1)} - (m+1)b^{-(m+2)} - ha^{-(m+1)}} \quad (6)$$

2.2 The problem formulation

Consider a radially polarized thick-walled FGPM sphere with perfect conductivity subjected to a uniform magnetic field vector $\vec{H}(0,0,H_\varphi)$. The components of the displacement, stress, radial electric displacement, electric potential, and perturbation of magnetic field vector in the spherical coordinate (r,θ,φ) are, respectively, expressed as $u(r)$, $\sigma_i(i=r,\theta,\varphi)$, D_r and $\phi(r)$. Due to symmetry, it is assumed that $U_\theta = U_\varphi = 0$, $\sigma_\theta = \sigma_\varphi$. The constitutive equations for the FGPM hollow sphere subjected to a rapid charge in temperature $T(r)$ are expressed as

$$\sigma_r = c_{11} \frac{\partial u}{\partial r} + 2c_{12} \frac{u}{r} + e_{11} \frac{\partial \phi(r)}{\partial r} - \lambda T(r), \quad (7a)$$

$$\sigma_\theta = c_{12} \frac{\partial u}{\partial r} + 2c_{22} \frac{u}{r} + e_{12} \frac{\partial \phi(r)}{\partial r} - \lambda T(r), \quad (7b)$$

$$D_r = e_{11} \frac{\partial u}{\partial r} + 2e_{12} \frac{u}{r} + g_{11} \frac{\partial \phi(r)}{\partial r} + p_{11} T(r) \quad (7c)$$

where $c_{ij}(i,j=1,2)$, $e_i(i=1,2)$, g_{11} , p_{11} and λ are elastic constants, dielectric constant, piezoelectric coefficient and thermal expansion coefficients, respectively, and all material constants are assumed to follow the same power-law function across the thickness of the FGPM hollow sphere, i.e.

$$\begin{aligned} c_{ij}(r) &= c_{ij}^0 r^m (i,j=1,2), & e_{ij}(r) &= e_{ij}^0 r^m (i,j=1,2), & g_{11}(r) &= g_{11}^0 r^m, \\ p_{11}(r) &= p_{11}^0 r^m, & \alpha(r) &= \alpha_i^0 r^m (i=1,2), & \mu(r) &= \mu_0 r^m, & c(r) &= c^0 r^m, \\ \lambda &= c(r) \alpha(r) = c^0 \alpha^0 r^{2m} = \lambda^0 r^{2m} \end{aligned} \quad (8)$$

where α is the thermal expansion constant. The mechanical and electrical boundary conditions are expressed as

$$\sigma_r|_{r=a} = -P_a, \quad \sigma_r|_{r=b} = -P_b, \quad \phi_r|_{r=a} = \phi_a, \quad \phi_r|_{r=b} = \phi_b \quad (9)$$

Assuming that the magnetic permeability, μ , at the outer surface of the FGPM sphere to be equal to the magnetic permeability of the medium around it, and omitting displacement electric currents, the governing electrostatics Maxwell equations for a perfectly conducting elastic body can be written as [12,13]

$$\vec{J} = \Delta \times \vec{h}, \quad \Delta \times \vec{e} = -\mu \frac{\partial \vec{h}}{\partial t}, \quad \text{div} \vec{h} = 0, \quad \vec{e} = -\mu \left(\frac{\partial \vec{U}}{\partial t} \times \vec{H} \right), \quad \vec{h} = \text{Curl}(\vec{U} \times \vec{H}) \quad (10)$$

where $\vec{J}, \vec{e}, \vec{H}, \vec{h}$ are the electric current density vector, perturbation of electric field vector, magnetic intensity vector and perturbation of magnetic field vector, respectively. In the spherical coordinates (r, θ, φ) , applying an initial magnetic field vector $\vec{H}(0, 0, H_\varphi)$ into Eq. (10) yields

$$\vec{U}(u, 0, 0), \quad \vec{e} = -\mu \left(0, H_\varphi \frac{\partial u}{\partial t}, 0 \right), \quad \vec{h} = (0, 0, h_\varphi), \quad \vec{J} = \left(0, -\frac{\partial h_\varphi}{\partial r}, 0 \right), \quad h_\varphi = -H_\varphi \left(\frac{\partial u}{\partial r} + \frac{2u}{r} \right) \quad (11)$$

In the absence of body force, the equilibrium equation of FGPM hollow sphere is expressed as [12, 13]

$$\frac{\partial \sigma_r}{\partial r} + \frac{2}{r}(\sigma_r - \sigma_\theta) + f_\varphi = 0 \quad (12)$$

where f_φ is the Lorentz's force [12, 13] which can be expressed as

$$f_\varphi = \mu(r)(\vec{J} \times \vec{H}) = \mu(r)H_\varphi^2 \frac{\partial}{\partial r} \left(\frac{\partial u}{\partial r} + \frac{2u}{r} \right) \quad (13)$$

In the absence of charge density force, the charge equation of electrostatics is expressed as [14]

$$\frac{\partial D_r}{\partial r} + \frac{2D_r}{r} = 0, \quad (a \leq r \leq b) \quad (14)$$

Solving Eq. (14) yields

$$D_r = \frac{A_1}{r^2} \quad (15)$$

Substituting Eqs. (8) and (15) into Eq. (7c) yields

$$\frac{\partial \phi(r)}{\partial r} = \frac{e_{11}^0}{g_{11}^0} \frac{\partial u}{\partial r} + \frac{2e_{12}^0}{g_{11}^0} \frac{u}{r} + \frac{p_{11}^0}{g_{11}^0} T(r) - \frac{A_1}{g_{11}^0} \frac{1}{r^{m+2}} \quad (16)$$

Substituting Eqs. (16) and (4) into Eqs. (7a) and (7b) and utilizing Eq. (8) yields

$$\sigma_r = w_1 r^m \frac{\partial u}{\partial r} + w_2 r^m \frac{u}{r} + w_3 r^{2m} + w_4 r^m + w_5 r^{m-1} + w_6 r^{-1} + w_7 r^{-2} A_1, \quad (17 a)$$

$$\sigma_{\theta} = w_8 r^m \frac{\partial u}{\partial r} + w_9 r^m \frac{u}{r} + w_3 r^{2m} + w_{10} r^m + w_5 r^{m-1} + w_{11} r^{-1} + w_{12} r^{-2} A_1 \quad (17b)$$

where

$$\begin{aligned} w_1 &= c_{11}^0 + \frac{(e_{11}^0)^2}{g_{11}^0}, & w_2 &= 2c_{12}^0 + \frac{2e_{11}^0 e_{12}^0}{g_{11}^0}, & w_3 &= -\lambda^0 c_2, & w_4 &= \frac{e_{11}^0 p_{11}^0}{g_{11}^0} c_2, \\ w_5 &= -\lambda^0 c_1, & w_6 &= \frac{e_{11}^0 p_{11}^0}{g_{11}^0} c_1, & w_7 &= -\frac{e_{11}^0}{g_{11}^0}, & w_8 &= c_{12}^0 + \frac{e_{11}^0 e_{12}^0}{g_{11}^0}, \\ w_9 &= c_{22}^0 + \frac{2(e_{12}^0)^2}{g_{11}^0}, & w_{10} &= \frac{e_{12}^0 p_{11}^0}{g_{11}^0} c_2, & w_{11} &= \frac{e_{12}^0 p_{11}^0}{g_{11}^0} c_1, & w_{12} &= -\frac{e_{12}^0}{g_{11}^0} \end{aligned} \quad (18)$$

2.3 The solution of equilibrium equation for FGPM

Substituting Eqs. (17a), (17b) and (13) into Eq. (12), the equilibrium equation of FGPM hollow sphere is expressed as

$$\frac{\partial^2 u}{\partial r^2} + z_1 \frac{1}{r} \frac{\partial u}{\partial r} + z_2 \frac{u}{r^2} = z_3 A_1 r^{-3-m} + z_4 r^{-2-m} + z_5 r^{m-1} + z_6 r^{-2} + z_7 r^{-1} \quad (19)$$

where

$$\begin{aligned} z_1 &= \frac{w_1(2+m) + \mu_0 H^2(2+m)}{w_1 + \mu_0 H^2}, & z_2 &= \frac{w_2(m+1) - 2w_9 + 2\mu_0 H^2(m-1)}{w_1 + \mu_0 H^2}, \\ z_3 &= \frac{2w_{12}}{w_1 + \mu_0 H^2}, & z_4 &= \frac{-w_6 + 2w_{11}}{w_1 + \mu_0 H^2}, & z_5 &= \frac{-2w_3 m}{w_1 + \mu_0 H^2}, \\ z_6 &= \frac{-w_5(m-1)}{w_1 + \mu_0 H^2}, & z_7 &= \frac{-w_4(m+2) + 2w_{10}}{w_1 + \mu_0 H^2} \end{aligned} \quad (20)$$

The solution of Eq. (19) can be written as

$$u(r) = u^h(r) + u^p(r) \quad (21)$$

where $u^h(r)$ and $u^p(r)$ are the homogeneous and particular solutions, respectively. The homogeneous solution of Eq. (19) is expressed as follows

$$u^h(r) = S r^n \quad (22)$$

where S is an arbitrary constant, substituting Eq. (22) into Eq. (19) yields

$$n^2 + (z_1 - 1)n + z_2 = 0 \quad (23)$$

The roots of the characteristics Eq. (23) are written as

$$n_{1,2} = \frac{1}{2}(1 - z_1 \pm \sqrt{(z_1 - 1)^2 - 4z_2}) \quad (24)$$

These roots may be real distinct, double roots, and complex conjugate. For real distinct roots, the solution of Eq. (22) is expressed as

$$u^h(r) = A_2 r^{n_1} + A_3 r^{n_2} \quad (25)$$

In the case of double roots, $n_1 = n_2 = n$ the solution of Eq. (22) is written as the following form

$$u^h(r) = (A_2 + A_3 \ln r) r^n \quad (26)$$

and the solution of Eq. (22) for complex roots $n_1 = x + yi, n_2 = x - yi$ is obtained as

$$u^h(r) = [A_2 \cos(y \ln r) + A_3 \sin(y \ln r)] r^x \quad (27)$$

where A_2 and A_3 are the unknown constants that determined by the given boundary conditions Eq. (9) for the real distinct roots and $-2 < m < 2$. The particular solution $u^p(r)$ to Eq. (19) can be obtained as

$$u^p(r) = Q_1 + Q_2 r + Q_3 A_1 r^{-m-1} + Q_4 r^{m+1} + Q_5 r^{-m} \quad (28)$$

Substituting Eq. (28) into Eq. (19) yields

$$\begin{aligned} \frac{\partial^2 u^p}{\partial r^2} + z_1 \frac{1}{r} \frac{\partial u^p}{\partial r} + z_2 \frac{u^p}{r^2} &= [(m+1)(m+2) - z_1(m+1) + z_2] Q_3 A_1 r^{-3-m} \\ &+ [m(m+1) - m z_1 + z_2] Q_5 r^{-2-m} + [(m+1)z_1 + z_2 + m(m+1)] Q_4 r^{m-1} \\ &+ z_2 Q_1 r^{-2} + (z_1 + z_2) Q_2 r^{-1} = z_3 A_1 r^{-3-m} + z_4 r^{-2-m} + z_5 r^{m-1} + z_6 r^{-2} + z_7 r^{-1} \end{aligned} \quad (29)$$

According to the coefficients of the identical powers, the coefficients are:

$$\begin{aligned} Q_1 &= \frac{z_6}{z_1}, \quad Q_2 = \frac{z_7}{z_1 + z_2}, \quad Q_3 = \frac{z_3}{[(m+1)(m+2) - z_1(m+1) + z_2]}, \\ Q_4 &= \frac{z_5}{[(m+1)z_1 + z_2 + m(m+1)]}, \quad Q_5 = \frac{z_4}{[(m+1) - z_1 m + z_2]} \end{aligned} \quad (30)$$

Substituting Eqs. (25) and (28) into Eq. (21) yields

$$u(r) = u^h(r) + u^p(r) = A_2 r^{n_1} + A_3 r^{n_2} + Q_1 + Q_2 r + Q_3 A_1 r^{-m-1} + Q_4 r^{m+1} + Q_5 r^{-m} \quad (31)$$

Substituting Eq. (31) into Eq. (16) yields

$$\begin{aligned} \frac{\partial \phi(r)}{\partial r} &= -w_7 [A_2 n_1 r^{n_1-1} + A_3 n_2 r^{n_2-1} + Q_2 + Q_3 A_1 (-m-1) r^{-m-2} + Q_4 (m+1) r^m \\ &+ Q_5 (-m) r^{-m-1}] - 2w_{12} [A_2 r^{n_1-1} + A_3 r^{n_2-1} + Q_1 r^{-1} + Q_2 + Q_3 A_1 r^{-m-2} \\ &+ Q_4 r^m + Q_5 r^{-m-1}] + \frac{p_{11}^0}{g_{11}^0} (c_1 r^{-m-1} + c_2) - \frac{A_1}{g_{11}^0} \frac{1}{r^{m+2}} \end{aligned} \quad (32)$$

Integrating Eq. (32) yields

$$\begin{aligned}
 \phi(r) = & -w_7[A_2r^{n_1} + A_3r^{n_2} + Q_2r + Q_3A_1r^{-m-1} + Q_4r^{m+1} + Q_5r^{-m}] - 2w_{12}\left[\frac{A_2}{n_1}r^{n_1} + \frac{A_3}{n_2}r^{n_2} + Q_1 \ln r \right. \\
 & \left. + Q_2r + \frac{Q_3}{(-m-1)}A_1r^{-m-1} + \frac{Q_4}{m+1}r^{m+1} + \frac{Q_5}{-m}r^{-m}\right] + \frac{p_{11}^0}{g_{11}^0}\left(\frac{c_1}{-m}r^{-m} + c_2r\right) - \frac{A_1}{g_{11}^0}\frac{1}{m+1}r^{-m-1} + A_4
 \end{aligned} \quad (33)$$

Substituting Eq.(31) into final item of Eq. (11) and Eqs. (17a) and (17b), the perturbation of magnetic field vector, radial and circumferential stresses of the FGPM hollow sphere are obtained as

$$\begin{aligned}
 \sigma_r = & w_1r^m(A_2n_1r^{n_1-1} + A_3n_2r^{n_2-1} + Q_2 + Q_3A_1(-m-1)r^{-m-2} + Q_4(m+1)r^m \\
 & + Q_5(-m)r^{-m-1}) + w_2r^m(A_2r^{n_1-1} + A_3r^{n_2-1} + \frac{Q_1}{r} + Q_2 + Q_3A_1r^{-m-2} \\
 & + Q_4r^m + Q_5r^{-m-1}) + w_3r^{2m} + w_4r^m + w_5r^{m-1} + w_6r^{-1} + w_7r^{-2}A_1
 \end{aligned} \quad (34a)$$

$$\begin{aligned}
 \sigma_\theta = & w_8r^m(A_2n_1r^{n_1-1} + A_3n_2r^{n_2-1} + Q_2 + Q_3A_1(-m-1)r^{-m-2} + Q_4(m+1)r^m \\
 & + Q_5(-m)r^{-m-1}) + w_9r^m(A_2r^{n_1-1} + A_3r^{n_2-1} + \frac{Q_1}{r} + Q_2 + Q_3A_1r^{-m-2} \\
 & + Q_4r^m + Q_5r^{-m-1}) + w_{10}r^m + w_5r^{m-1} + w_{11}r^{-1} + w_{12}r^{-2}A_1
 \end{aligned} \quad (34b)$$

$$\begin{aligned}
 h_\phi = & -H_\phi\left(\frac{\partial u}{\partial r} + \frac{u}{r}\right) = -H_\phi\left[(n_1+2)A_2r^{n_1-1} + (n_2+2)A_3r^{n_2-1} + \frac{2Q_1}{r} + 3Q_2 \right. \\
 & \left. + (-m+1)Q_3A_1r^{-m-2} + (m+3)Q_4r^m + (-m+2)Q_5r^{-m-1}\right]
 \end{aligned} \quad (34c)$$

where A_1, A_2, A_3 and A_4 are unknown constants that determined by the given boundary conditions.

3 NUMERICAL RESULTS AND DISCUSSIONS

In this article, electro-magneto-thermo-mechanical stresses, electric displacement, electric potential and perturbation of magnetic field vector of the FGPM hollow sphere under electric, thermal and mechanical loads are considered to determine a numerical result. The mechanical, electrical, magnetic and thermal constants for the FGPM hollow sphere are considered as [9, 11, and 15]

$$\begin{aligned}
 c_{11}^0 &= 1.5 \times 10^{11} \text{ Pa}, \quad c_{12}^0 = 7.4 \times 10^{10} \text{ Pa}, \quad c_{22}^0 = 2.2 \times 10^{11} \text{ Pa}, \\
 e_{11}^0 &= 15.1 \text{ C/m}^2, \quad e_{12}^0 = -5.2 \text{ C/m}^2, \quad g_{11}^0 = -5.62 \times 10^{-9} \text{ C}^2/\text{Nm}^2, \\
 c^0 &= 500 \text{ GPa}, \quad p_{11}^0 = -2.5 \times 10^{-5} \text{ C/m}^2\text{K}, \quad \mu_0 = 4\pi \times 10^{-7} \text{ H/m}, \\
 H_\phi &= 2.23 \times 10^9 \text{ A/m}, \quad h = 0.72 \text{ W/mK}, \quad \alpha^0 = 1.2 \times 10^{-6} \text{ 1/K}
 \end{aligned} \quad (35)$$

The non-dimensional parameters are defined as

$$R = \frac{r-a}{b-a}, \quad T^* = \frac{T(r)}{T_o}, \quad \sigma_i^* = \frac{\sigma_i}{P_a} \quad (i = r, \theta), \quad \phi^* = \frac{\phi(r)}{\phi_a}, \quad h_\phi^* = \frac{h_\phi}{H_\phi} \quad (36)$$

Example 1.

In this example, a thick hollow sphere is considered that the geometry parameters and boundary conditions and the corresponding boundary conditions are expressed as

$$P_a = 1 \times 10^7 \text{ Pa}, P_b = 0, \phi_a = 50 \text{ W/A}, \phi_b = 0, a = 0.25 \text{ m}, b = 0.5 \text{ m}, T|_{r=a} = 300^\circ \text{ K} \quad (37)$$

Fig. 1 shows the variation of temperature along the radial direction for different values of the material parameter m . It is seen from the results that the non-dimensional temperature at the inner radius equals one, which satisfies prescribed thermal boundary condition, and the non-dimensional temperature decreases with increasing the power law index m at the same radial point of the FGPM hollow sphere. Also, it is observed from this figure that variation of non-dimensional temperature is approximately constant with increasing non dimensional radius. The variation of the non-dimensional electric displacement distribution along the radial direction of the FGPM hollow sphere for different values of material parameters m are demonstrated in Fig. 2. It can easily be seen from the curves that for a specific value of the position parameter r , the absolute non-dimensional electric displacement decreases with increasing the material parameter m . It is also seen that the absolute value of non-dimensional electric displacement decreases from the internal to external surface of the FGPM hollow sphere.

Figs. 3 and 4 depict the distribution of non-dimensional radial and circumferential stresses along the radius for different values of material parameters, respectively. It is seen from the Fig. 3 that the non-dimensional radial stresses at the internal and external surfaces of the FGPM hollow sphere satisfy the given boundary conditions. The variation of absolute non-dimensional radial stress decreases with increasing m . Also, this value increases with increasing non-dimensional radius. As can be seen from Fig. 3, the non-dimensional radial stress distributions are in good agreement with those of [9]. Hence, the correctness of the present solution can therefore be verified in this respect, too. It is seen from Fig. 4 that a positive m has more apparent effect on the distributions of non-dimensional circumferential stresses. Also, the non-dimensional circumferential stress decreases with increasing non-dimensional radius for a positive m .

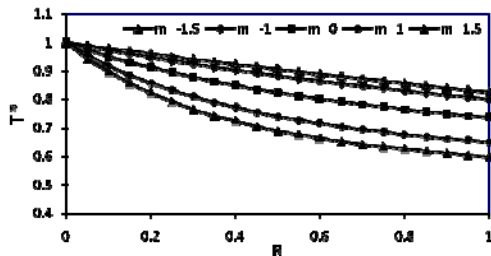


Fig. 1
Temperature distributions in FGPM hollow sphere with various amounts of m , where $a = 0.25m, b = 0.5m$ and $T_0 = 300K$.

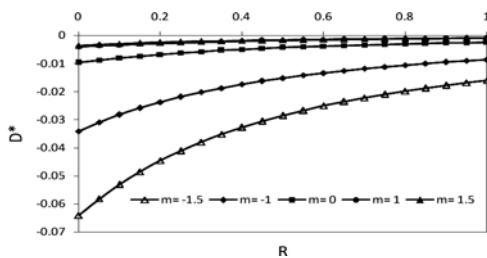


Fig. 2
Electric displacement distributions in FGPM hollow sphere with various amounts of m , where $a = 0.25m, b = 0.5m$ and $T_0 = 300K$.

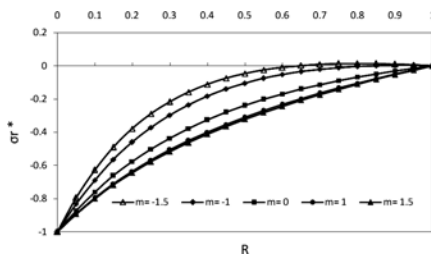


Fig. 3
Radial stress distributions in FGPM hollow sphere with various amounts of m , $a = 0.25m, b = 0.5m$ and $T_0 = 300K$.

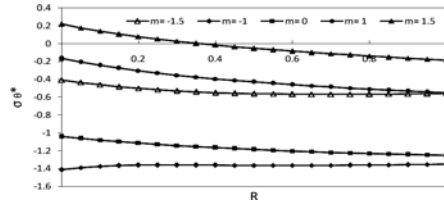


Fig. 4
Circumferential stress distributions in FGPM hollow sphere with various amounts of m , $a = 0.25m$, $b = 0.5m$ and $T_0 = 300K$.

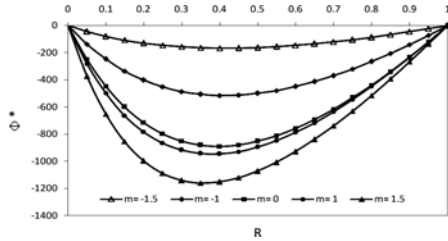


Fig. 5
Electric potential distributions in FGPM hollow sphere with various amounts of m , $a = 0.25m$, $b = 0.5m$ and $T_0 = 300K$.

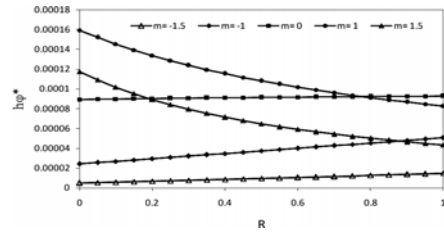


Fig. 6
Perturbation of magnetic field vector distributions in FGPM hollow sphere with various amounts of m , $a = 0.25m$, $b = 0.5m$ and $T_0 = 300K$.

Figs. 5 and 6 show the non-dimensional electric potential and perturbation of magnetic field vector distributions in the FGPM hollow sphere, respectively. From Fig. 5 one knows, the non-dimensional electric potential satisfies the electric boundary condition and the absolute values of non-dimensional electric potential increases with increasing of material property m . Also, it is observed from the results that the maximum value of the absolute non-dimensional electric potential is at range 0.3 to 0.5 of non-dimensional radius. Fig. 6 shows that for any negative or zero material parameters m , the perturbation of magnetic field vector distributions increases almost linearly along the thickness. But for any positive material parameters m , the perturbation of magnetic field vector distributions decreases along the thickness of FGPM sphere nonlinearly.

Example 2.

Considering electro-magneto-thermo-elastic stresses, electric potential, and perturbation of magnetic field vector of the FGPM hollow sphere at different thermal boundary condition T_0 the inner radius $a = 0.1$ m, outer radius $b = 0.2$ m and $m=1$ is considered and all other conditions are similar to example 1. Figs.7-10 show the non-dimensional perturbation of magnetic field vector, electric potential, radial and circumferential stresses of the proposed FGPM hollow sphere for various temperatures. Fig.7. shows that the non-dimensional perturbation of magnetic field vector at the same radial point decreases with increase of the temperature. Also, it is seen that non-dimensional perturbation of magnetic field vector is maximum at internal surface. It can be concluded from Fig.8. that the electric potential completely satisfies the electric boundary conditions and its trend is similar to Fig. 5. Fig. 9 shows the variation of non-dimensional radial stress along the thickness of the FGPM hollow sphere which satisfies the given mechanical boundary conditions and increases by increasing the temperature. It is found that the effect of temperature on non-dimensional radial stress is significant. Fig. 10 demonstrates that the non-dimensional circumferential stresses decreases in a specific radius by increasing the temperature and for $T_0 = 500^\circ K$ the non-dimensional circumferential stress is negatively increased.

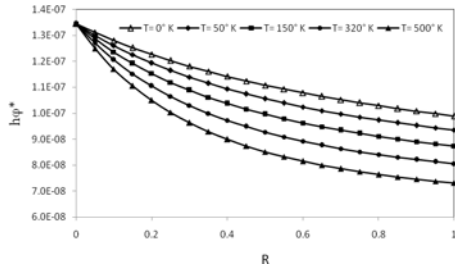


Fig. 7
 Perturbation of magnetic field vector distributions in FGPM hollow sphere with various amounts of T , where $a = 0.25m$, $b = 0.5m$ and $T_0 = 300K$.

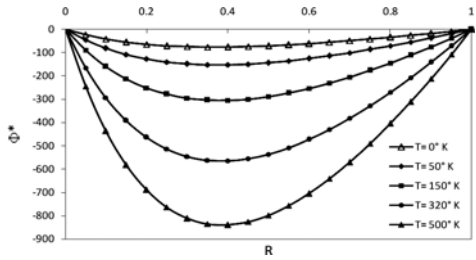


Fig. 8
 Electric potential distributions in FGPM hollow sphere with various amounts of T , where $a = 0.25m$, $b = 0.5m$ and $T_0 = 300K$.

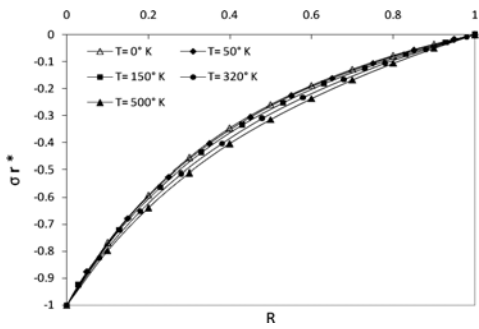


Fig. 9
 Radial stress distributions in FGPM hollow sphere with various amounts of T , where $a = 0.25m$, $b = 0.5m$ and $T_0 = 300K$.

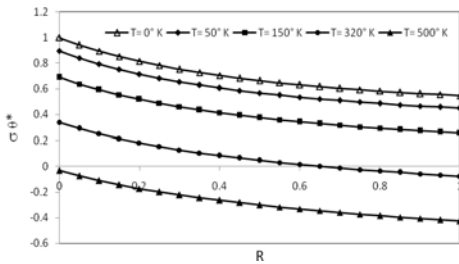


Fig. 10
 Circumferential stress distributions in FGPM hollow sphere with various amounts of T , where $a = 0.25m$, $b = 0.5m$ and $T_0 = 300K$.

4 CONCLUSIONS

Analytical solution for a FGPM hollow sphere in a uniform magnetic field, subjected to thermal, electrical and mechanical loads are obtained. All material parameters except Poisson's ratio are assumed to have the same exponent-low dependence on the radial direction of the FGPM hollow sphere. The results show that the gradient index m and temperature have a significant effect on the electro-magneto-thermo-mechanical stresses, perturbation of the magnetic field vector, and electric potential and hence should be considered in optimum design. This is to say, the in-homogeneous constants presented here are useful parameters from a design point of view in that they can be tailored for specific applications to control the distributions of electro-magneto-thermo-mechanical stresses. The

technological implications of this study could be significant in applications such as reduction or neutralization of hoop stress resulting from electro-magneto-thermo-mechanical loads in a FGPM hollow sphere by a suitably applied electric field and material in-homogeneity.

REFERENCES

- [1] Chen W.Q., Lu Y., Ye J. R., Cai J.B., 2002, 3D electroelastic fields in a functionally graded piezoceramic hollow sphere under mechanical and electric loading, *Archive of Applied Mechanics* **72**: 39-51.
- [2] Lim C.W., He L.H., 2001, Exact solution of a compositionally graded piezoelectric layer under uniform stretch, bending and twisting, *International Journal of Mechanical Sciences* **43**: 2479-2492.
- [3] Shi Z. F., Chen Y., 2004, Functionally graded piezoelectric cantilever beam under load, *Archive of Applied Mechanics* **74**: 237-247.
- [4] Wu C. P., Syu Y.S., 2007, Exact solution of functionally graded piezoelectric shells under cylindrical bending, *International Journal of Solids and Structures* **44**: 6450-6472.
- [5] Dai H.L., Fu Y.M., Yang J.H., 2007, Electromagnetoelastic behaviors of functionally graded piezoelectric solid cylinder and sphere, *Acta Mechanica Sinica* **23**: 55-63.
- [6] Ootao Y., Tanigawa Y., 2007, Transient piezothermoelastic analysis for a functionally graded thermopiezoelectric hollow sphere, *Composite Structures* **81**: 540-549.
- [7] Khoshgoftar M.J., Ghorbanpour Arani A., Arefi M., 2009, Thermoelastic analysis of a thick walled cylinder made of functionally graded piezoelectric material, *Smart Materials and Structures* **18**: 115007.
- [8] Ghorbanpour Arani A., Loghman A., Abdollahitaheri A., Atabakhshian V., 2010, Electro-thermo-mechanical behaviors of a radially polarized rotating functionally graded piezoelectric cylinder, *Journal of Mechanics of Materials and Structures*, in press.
- [9] Ghorbanpour Arani A., Salari M., Khademizadeh H., Arefmanesh A., 2010, Magneto-thermoelastic stress and perturbation of magnetic field vector in a functionally graded hollow sphere, *Archive of Applied Mechanics* **80**: 189-200.
- [10] Ghorbanpour Arani A., Salari M., Khademizadeh H., Arefmanesh A., 2009, Magneto-thermoelastic transient response of a functionally graded thick hollow sphere subjected to magnetic and thermoelastic fields, *Archive of Applied Mechanics* **79**: 481-497.
- [11] Dai H.L., Hong L., Fu Y.M., Xiao X., 2010, Analytical solution for electromagneto-thermoelastic behaviors of a functionally graded piezoelectric hollow cylinder, *Applied Mathematical Modelling* **34**: 343-357.
- [12] Kraus J.D., 1984, *Electromagnetic*, McGraw-Hill, New York.
- [13] Dai H.L., Wang X., 2004, Dynamic responses of piezoelectric hollow cylinders in an axial magnetic field, *International Journal of Solids and Structures* **41**: 5231-5246.
- [14] Heyliger P., 1996, A note on the static behavior of simply supported laminated piezoelectric cylinders, *International Journal of Solids and Structures* **34**: 3781-3794.
- [15] Wang H.M., Xu Z.X., 2010, Effect of material inhomogeneity on electromechanical behaviors of functionally graded piezoelectric spherical structures, *Computational Materials Science* **48**: 440-445.